



22

## 23 **Abstract**

24 The seasonal influenza vaccine is an important public health tool but is only effective in a subset of  
25 individuals. The identification of molecular signatures provides a mechanism to understand the drivers of  
26 vaccine-induced immunity. Most previously reported molecular signatures of influenza vaccination were  
27 derived from a single age group or season, ignoring the effects of immunosenescence or vaccine  
28 composition. Thus, it remains unclear how immune signatures of vaccine response change with age across  
29 multiple seasons. Here we profile the transcriptional landscape of young and older adults over five  
30 consecutive vaccination seasons to identify shared signatures of vaccine response as well as marked  
31 seasonal differences. Along with substantial variability in vaccine-induced signatures across seasons, we  
32 uncovered a common transcriptional signature 28 days post-vaccination in both young and older adults.  
33 However, gene expression patterns associated with vaccine-induced antibody responses were distinct in  
34 young and older adults; for example, increased expression of Killer Cell Lectin Like Receptor B1 (*KLRB1*;  
35 *CD161*) 28 days post-vaccination positively and negatively predicted vaccine-induced antibody responses  
36 in young and older adults, respectively. These findings contribute new insights for developing more  
37 effective influenza vaccines, particularly in older adults.

38

## 39 **Keywords**

40 systems vaccinology; seasonal variability; influenza; vaccination; aging; transcriptional profiling

41

42

## 43 **Introduction**

44 Influenza is a major public health burden, particularly in high-risk populations such as older adults. The  
45 seasonal inactivated influenza vaccination (IIV) is estimated to be 50-70% effective in randomized  
46 controlled trials of young adults (1–5), and efficacy is reduced to under 50% in adults over age 65 (6).  
47 Understanding the dynamics of vaccination-induced immune responses, and the factors associated with  
48 immunological protection should provide insights important for improving vaccine design.

49  
50 Systems vaccinology approaches utilizing high-throughput immune profiling techniques have identified  
51 signatures of response to influenza vaccination (7–14). These include pre-vaccination transcriptional  
52 signatures of apoptosis-related gene modules (9), as well as B cell signaling and inflammatory modules  
53 (15). Post-vaccination transcriptional signatures have also been identified, including an early interferon  
54 response 1 day post-vaccination and a plasma cell response 3 and 7 days post-vaccination (13). Interferon  
55 stimulated genes were upregulated in both monocytes and neutrophils between 15 and 48 hours post-  
56 vaccination and correlated with influenza-specific antibody responses (7, 12). In addition, the expression  
57 of genes enriched for proliferation and immunoglobulin production 7 days post-vaccination accurately  
58 predicted antibody response in an independent cohort (10). Studies of the influence of aging revealed that  
59 an early interferon response 1-2 days post-vaccination as well as an oxidative phosphorylation and plasma  
60 cell response 7 days post-vaccination were correlated with antibody response in young adults but were  
61 diminished or dysregulated in older adults (13, 14).

62  
63 Notably, previous studies of influenza vaccine response studying the effects of aging used data from a  
64 single vaccine season (9) or from two consecutive seasons in which vaccine composition was identical  
65 (13, 14); consequently, the generalizability of these signatures is unknown. To date, no comprehensive  
66 characterization of vaccine response in both young and older adults has been reported to multiple  
67 influenza vaccines which vary in composition. To address this gap, we profiled young and older adults  
68 over five consecutive vaccination seasons (2010-11, 2011-12, 2012-13, 2013-14, and 2014-15) hereafter  
69 referred to by the first year of each season. We developed a new automated metric to quantify antibody  
70 response while accounting for baseline titers and used this novel metric to identify predictive  
71 transcriptional signatures of vaccine response using post-vaccination as well as baseline gene expression  
72 profiles.

73

74

## 75 **Materials and Methods**

76

### 77 ***Clinical Study Design and Specimen Collection***

78 A total of 317 subjects were recruited at Yale University over the five vaccination seasons between 2010  
79 and 2014 and HAI titers pre- (D0) and post-vaccination (D28) were available from the 294 subjects  
80 reported in [Table 1](#). Informed consent was obtained for all subjects under a protocol approved by the  
81 Human Subjects Research Protection Program of the Yale School of Medicine. Participants with an acute  
82 illness two weeks prior to recruitment were excluded from the study, as were individuals with primary or  
83 acquired immune-deficiency, use of immunomodulating medications including steroids or chemotherapy,  
84 a history of malignancy other than localized skin or prostate cancer, or a history of cirrhosis or renal  
85 failure requiring hemodialysis. Blood samples were collected into Vacutainer sodium heparin tubes and  
86 serum tubes (Becton Dickinson) at four different time points, immediately prior to administration of  
87 vaccine (D0) and on D2 (2011, 2012, 2013, 2014) or D4 (2010), D7, and D28 post-vaccination.

88

89 In order to understand the transcriptional program underlying a successful vaccination response, we  
90 identified a subset of 134 subjects with extreme (strong or weak) antibody responses to perform  
91 transcriptional profiling by microarrays. In the first three seasons, the selection criteria were a four-fold  
92 increase to at least 2 strains (strong response) or no four-fold increase to any strain (weak response) as  
93 described previously (14). In the fourth and fifth seasons, the adjMFC metric was used in addition to the  
94 fold change criteria to account for baseline titers (11). The maxRBA response endpoint was developed  
95 after the study completed, however, less than 10% (12/134) of subjects chosen for transcriptional  
96 profiling had indeterminate responses by maxRBA (neither high or low responders using a 40% cutoff)  
97 ([Table 1](#)). These 12 subjects were excluded from the predictive modeling of antibody response.

98

### 99 ***HAI and VNA Analyses, Cell Sorting, RNA processing and Gene Expression Analyses***

100 Detailed methods are provided in *SI Appendix*.

101

## 102 Results

103

### 104 *Antibody Titer Dynamics*

105

106 We evaluated 294 healthy young (21 - 30 years old, n = 147) and older ( $\geq 65$  years old, n = 147) adults  
107 over five consecutive influenza vaccination seasons from 2010-2014. All subjects received the standard  
108 dose trivalent (2010, 2011, 2012) or quadrivalent (2013, 2014) seasonal inactivated influenza vaccine  
109 (IIV). We measured influenza-specific hemagglutination inhibition (HAI) titers pre-vaccination (D0) and  
110 28 days post-vaccination (D28). Over the course of our study, the vaccine composition changed relative  
111 to the previous season in three of five seasons ([Table 1](#)).

112

113 In all seasons, pre-vaccination titers were negatively correlated with the increase in titers post-vaccination  
114 (*SI Appendix*, Fig. S1). Previous work defined an adjusted maximum fold change (adjMFC) endpoint that  
115 removes the nonlinear correlation between fold change and baseline titers (11). However, adjMFC  
116 separates subjects into manually defined bins, making it difficult to perform high-throughput analysis.  
117 Furthermore, adjMFC does not allow for information sharing between bins as each bin is adjusted  
118 independently. To address these limitations, we developed maximum Residual after Baseline Adjustment  
119 (maxRBA), which corrects for the dependence on baseline titers for each strain by modeling titer fold  
120 changes as an exponential function of pre-vaccination titers and selecting the maximum residual across  
121 strains ([Fig. 1A](#)). All vaccine strains were approximately equally responsible for the maximum residual in  
122 any given season. “High responders” (HR) and “low responders” (LR) were defined as the top and bottom  
123 40th percentiles of the residuals, respectively. maxRBA can be interpreted as the maximum change from  
124 expected fold change given the initial titer; it is fully automated, is strain agnostic, and is correlated with  
125 plasmablast frequencies seven days post-vaccination (*SI Appendix*, Fig. S2A-B). Thus, maxRBA allows a  
126 completely automated assessment of the relative strength of each subject’s antibody response independent  
127 of pre-existing antibody titers.

128

129 Older adults had significantly lower pre-vaccination titers than young adults for three of five seasons ([Fig.](#)  
130 [1B](#)). The maximum fold change to any vaccine strain showed an increasing trend in young adults  
131 compared to older adults (*SI Appendix*, Fig. S3C). Because of the inverse relationship between baseline  
132 titers and fold change (*SI Appendix*, Fig. S1), we adjusted for baseline titers using maxRBA and found  
133 that the difference in vaccine response between young and older adults was statistically significant in  
134 more seasons ([Fig. 1C](#)). Males and females had similar pre-vaccine geometric mean titers (preGMTs) (*SI*  
135 *Appendix*, Fig. S3A). However, the antibody response calculated by maxRBA showed a trend toward  
136 stronger antibody responses in females compared to males with similar baseline titers in both age groups  
137 (Fisher’s combined  $p = 0.02$  (Young),  $p = 0.12$  (Older); *SI Appendix*, Fig. S3B). We did not detect any  
138 significant difference in baseline titers or titer responses across seasons when stratifying subjects by body  
139 mass index, smoking history, aspirin use, or diabetes medication use ( $p > 0.05$  two-sided Wilcoxon rank  
140 sum test (discrete) or simple linear regression (continuous)).

141

142

143

144

145

146 **Table 1**  
147 **Vaccine Compositions and Cohorts**

	<b>2010-11</b>	<b>2011-12</b>	<b>2012-13</b>	<b>2013-14</b>	<b>2014-15</b>
<b>Vaccine Composition<sup>a</sup></b>	A/California/7/2009	A/California/7/2009	A/California/7/2009	A/California/7/2009	A/California/7/2009
	A/Perth/16/2009	A/Perth/16/2009	A/Victoria/361/2011	A/Texas/50/2012	A/Texas/50/2012
	B/Brisbane/60/2008	B/Brisbane/60/2008	B/Wisconsin/1/2010	B/Brisbane/60/2008	B/Brisbane/60/2008
			B/Massachusetts/2/2012	B/Massachusetts/2/2012	
<b>Subjects</b>	42	69	92	56	35
<b>Gender (% Male)</b>	33	42	40	36	51
<b>Age Group (% Older)</b>	48	54	49	52	46
<b>Transcriptomes<sup>b</sup></b>	19	39	30	26	20
<b>Young (LR   I   HR)<sup>c</sup></b>	4   1   6	8   2   6	6   0   9	6   2   5	4   2   5
<b>Older (LR   I   HR)<sup>c</sup></b>	5   0   3	11   5   7	7   0   8	7   0   6	2   0   7

148 <sup>a</sup> The three vaccine strains in 2009-10 were A/Brisbane/59/2007, A/Brisbane/10/2007, and B/Brisbane/60/2008. A monovalent  
149 A/California/7/2009 vaccine was administered to some subjects in March 2010.

150 <sup>b</sup> Subjects with transcriptional data are a subset of subjects with antibody titers.

151 <sup>c</sup> Subjects are listed by antibody response category: low responder (LR), indeterminate (I), high responder (HR).

152  
153 We also examined the dynamics of viral titers over the course of the five seasons (*SI Appendix*, Fig. S3D).  
154 The A/California 7/2009 H1N1 strain was introduced into the seasonal vaccine in 2010 and remained  
155 through the 2014 season; however, pre-vaccine titers to this strain were consistently lower in older vs.  
156 young adults for 2011-2014. While we did not follow the same subjects across multiple seasons, 50-80%  
157 of young and 80-98% of older adults self-reported receiving influenza vaccine in the previous year. Taken  
158 together, these results support existing evidence that the capability for antibody persistence is reduced  
159 with age (16).

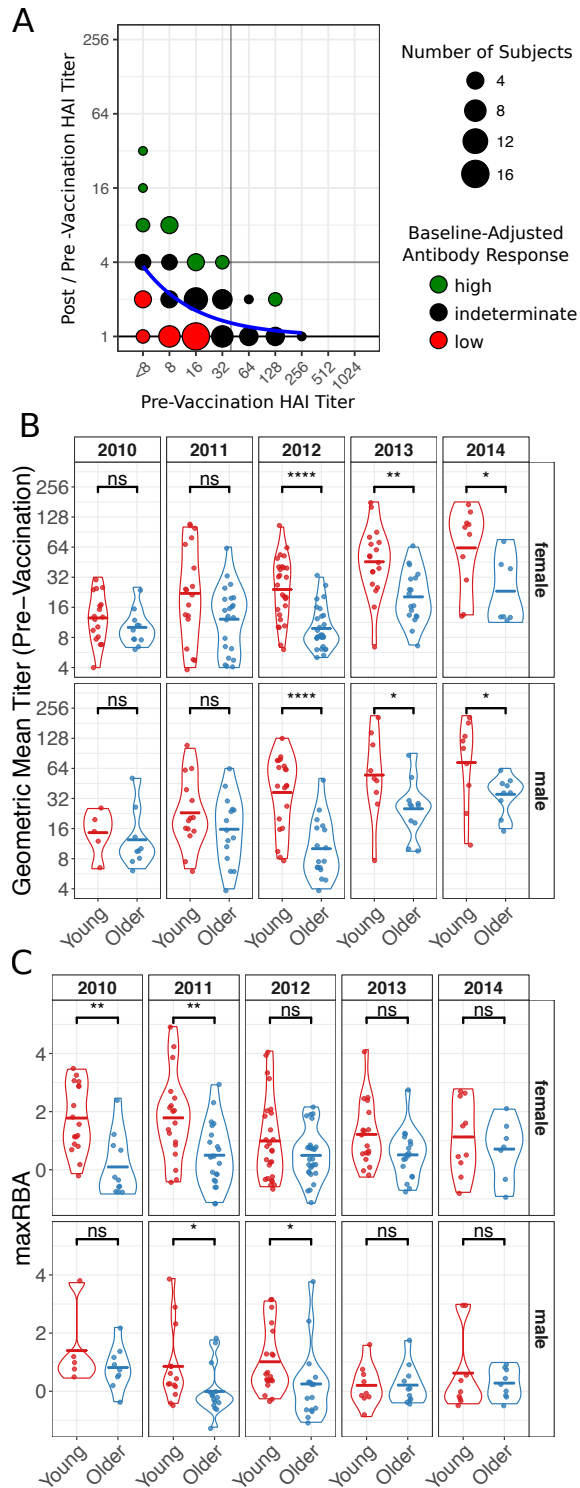
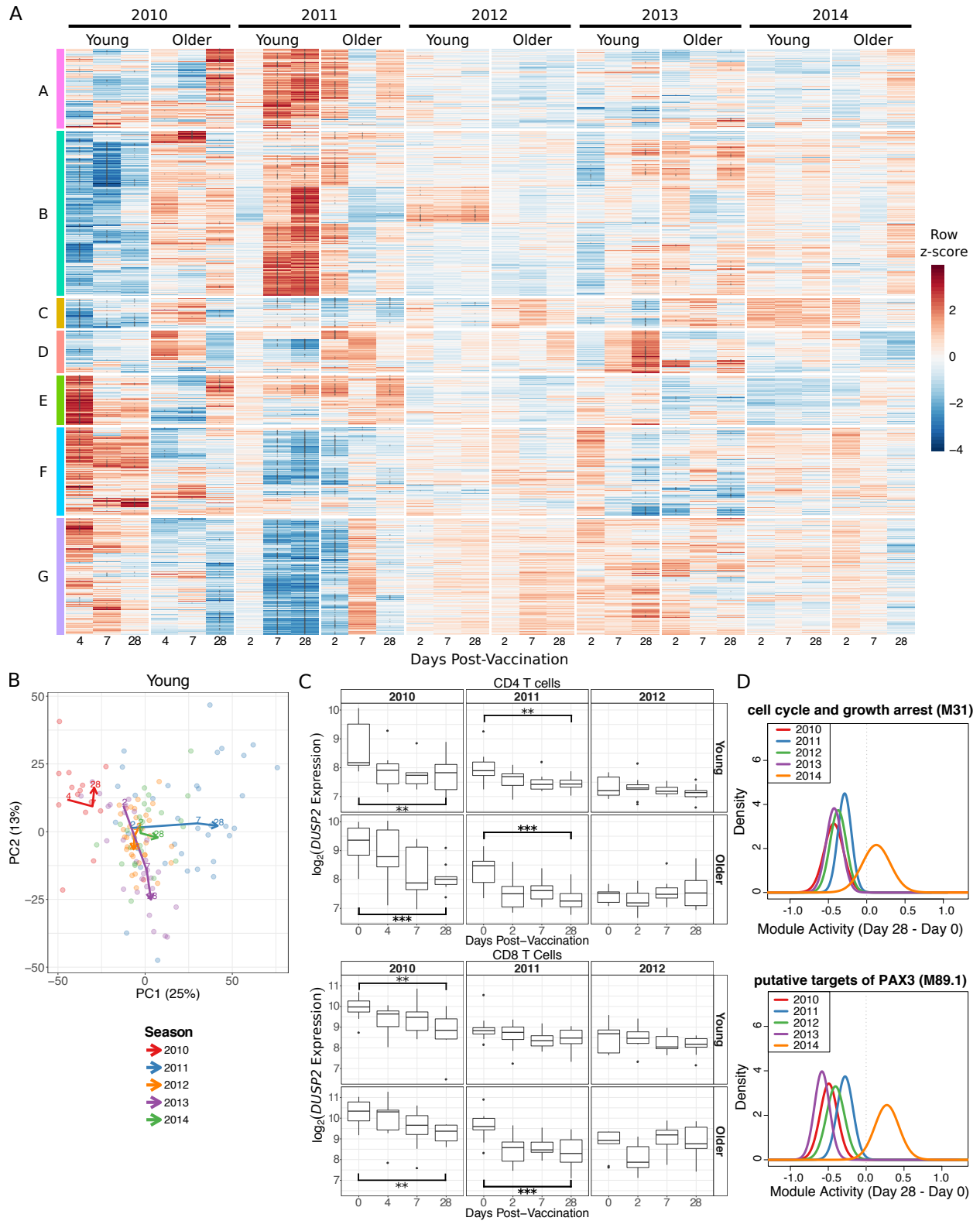


**Figure 1**

**Influenza-Specific Antibody Titers.** (A) An illustration of the maximum Residual after Baseline Adjustment (maxRBA) method for hemagglutination inhibition (HAI) titers to the B/Wisconsin/1/2010 strain in the 2012 season. An exponential curve (blue) is fit to the data and the residual is used to stratify subjects into high and low responders. Subjects with largest positive residuals are high responders (green) and subjects with smallest negative residuals are low responders (red). maxRBA is calculated using the maximum residual across all vaccine strains. (B and C) Violin plots of pre-vaccination HAI titers (B) and HAI responses measured by maxRBA (C) are separated by season and gender to compare age groups. Crossbars indicate the mean. Not Significant (ns)  $p > 0.05$ , \*  $p < 0.05$ , \*\*  $p < 0.01$ , \*\*\*  $p < 0.001$ , \*\*\*\*  $p < 0.0001$  independent two-sided Wilcoxon rank sum test.

1  
2  
3  
4  
5  
6



7  
8 **Figure 2**  
9 **Substantial Seasonal Variability in Signatures Induced by Influenza Vaccination.** (A) A row-  
10 normalized heatmap of the 2,462 significantly differentially expressed genes (DEGs). Clusters A-G were  
11 defined by hierarchical clustering. Asterisks within the heatmap indicate genes significantly differentially



12 expressed compared to day 0. (B) The first two principal components from a principal component  
13 analysis of all DEGs. Each point is a sample and lines connect the median of the points at each day post-  
14 vaccination within each season. (E) *DUSP2* expression in sorted CD4 and CD8 T cells. \*\*  $p < 0.01$ , \*\*\*  $p$   
15  $< 0.001$  one-sided t-test comparing day 28 and day 0 only. (F) Probability density functions calculated by  
16 QuSAGE for two representative gene modules significantly downregulated 28 days post-vaccination in  
17 four seasons. M31 contains *DUSP1* while M89.1 contains both *DUSP1* and *DUSP2*.

18  
19

## 20 ***Substantial Seasonal Variability in Vaccine-Induced Signatures***

21

22 To identify correlates and predictors of vaccine response, we selected a subset of individuals (20 - 40  
23 subjects per season) from young and older adult cohorts who had strong or weak antibody responses  
24 according to HAI titers and performed longitudinal transcriptional profiling pre-vaccination (baseline)  
25 and 4 (2010 cohort) or 2 days (all other cohorts), 7 days, and 28 days post-vaccination ([Table 1](#);  
26 [Methods](#)). We first performed differential expression analysis independently in each season without  
27 differentiating subjects by antibody response. We compared each post-vaccination time point to baseline  
28 and found a vaccine-induced signature that comprised a total of 2,462 significantly differentially  
29 expressed genes (DEGs) over all five seasons (FDR  $< 0.05$ , Fold Change  $> 1.25$ ; *SI File 1*).

30

31 Most of the DEGs were from the first two seasons whereas vaccination in the latter three seasons induced  
32 relatively weak changes ([Fig. 2A](#); *SI Appendix*, Fig. S4E). In fact, a substantial fraction of DEGs were  
33 unique to a single season and not differentially expressed at any time point in another season (Young:  
34 38%, Older: 75%). In young adults, there were 1,330 DEGs shared across two or more seasons while in  
35 older adults there were 265 shared DEGs. In both young and older adults, a substantial fraction of these  
36 shared genes was differentially expressed 28 days post-vaccination (*SI Appendix*, Fig. S4F). To assess  
37 whether vaccine-induced changes were consistent between seasons, we divided the 2,462 DEGs into 7  
38 clusters by hierarchical clustering ([Fig. 2A](#); *SI File 2*) and tested for their activity in every season using  
39 QuSAGE (17) (*SI Appendix*, Fig. S5). In young adults, three of the clusters (B, F, G) had significant, but  
40 opposite, activity during the 2010 and 2011 seasons, while these clusters were relatively consistent across  
41 seasons in older adults. Genes in cluster A were induced strongly in the 2011 season in both age groups  
42 and notably enriched for multiple pathways related to mitochondria, including *mitochondrial inner*  
43 *membrane, oxidative phosphorylation, respiratory electron transport, citric acid (TCA) cycle and*  
44 *respiratory electron transport, and mitochondrial respiratory chain complex assembly* (FDR  $< 0.05$ ; *SI*  
45 *File 2*). These findings reflect our previous identification of a mitochondrial biogenesis signature  
46 associated with influenza vaccine antibody response (14). Cluster D was only significantly induced in the  
47 2013 season at 7 and 28 days post-vaccination and was not significantly enriched for any gene sets tested  
48 (FDR  $> 0.05$ ; *SI File 2*). The cluster with the most consistent expression pattern across the five seasons  
49 was cluster C, which was enriched for pathways related to Toll-like receptor signaling, B and T cell  
50 signaling, NF- $\kappa$ B signaling, MAPK signaling, cell senescence or proliferation, and apoptosis (*SI File 2*).  
51 Interestingly, cluster C contains three genes (*DUSP1*, *DUSP2*, *CCL3L3*) which were significantly  
52 downregulated 28 days post-vaccination in four of five seasons. *CCL3L3* is a ligand for *CCR1*, *CCR3* and  
53 *CCR5*, known to be chemotactic for monocytes and lymphocytes (18). *DUSP1* and *DUSP2* are dual  
54 specificity phosphatases; *DUSP2* dephosphorylates *STAT3*, leading to inhibition of survival and  
55 proliferation signals (19–21), and an age-associated decrease in *DUSP1* function contributed to

56 inappropriate IL-10 production in monocytes before and after influenza vaccination (22). To determine  
57 whether downregulation of these three genes was a result of changes in cell subset composition or  
58 observed in subpopulations of cells, we performed transcriptional profiling on sorted B and T cells in a  
59 subset of individuals from three seasons. *DUSP1* and *DUSP2*, but not *CCL3L3*, were significantly  
60 downregulated 28 days post-vaccination over multiple seasons in CD4 and CD8 T cells of young adults  
61 (One sided t-test  $p < 0.01$ ; Fig. 2C, SI Appendix, Fig. S4C-D). Furthermore, while *DUSP2* was only  
62 significantly decreased in PBMCs of older individuals in the 2011 season, expression of *DUSP2* was  
63 significantly decreased 28 days post-vaccination in sorted CD4 and CD8 T cells from older individuals in  
64 multiple seasons (Fig. 2C). Thus, the downregulation of *DUSP2* 28 days post-vaccination is observed in  
65 the T cell compartment of both young and older adults.

66  
67 To further assess shared patterns in vaccine-induced changes across five seasons, we performed a  
68 principal component analysis (PCA) on gene expression fold changes post-vaccination for all DEGs. The  
69 first two components together explained 38% of the variation in young adults' and 46% of the variation in  
70 older adults' transcriptional changes post-vaccination (Fig. 2B, SI Appendix, Fig. S4B). Notably, in young  
71 adults, the 2011 and 2014 seasons (both with vaccine composition identical to the previous year) had  
72 similar trajectories, increasing along the first principal component (PC1) by D28 post-vaccine. Examining  
73 the genes contributing to PC1 reveals that four of the top 10 genes (*SLMAP*, *MATR3*, *MBNL3*, *RANBP3*)  
74 increase in expression post-vaccination more in the 2011 and 2014 seasons than in any other season. The  
75 shared trajectories along PC1 are not significantly enriched for any blood transcription modules (BTMs)  
76 (23), KEGG pathways (24), or cell subset signatures (25) (FDR  $> 0.05$ ; SI File 3). The trajectory of the  
77 2010 season was quite distinct from the other seasons in young adults. This season is consistently  
78 elevated on PC2, which is significantly enriched for monocytes, TLRs and inflammatory signaling (FDR  
79  $< 0.05$ ; SI File 3). The 2012 and 2013 seasons also appear to have similar trajectories, both decreasing in  
80 PC2 over time. The vaccines used in these two seasons each introduced multiple new strains while  
81 retaining the A/California/7/2009 strain. Five of the top 10 genes (*ZNF493*, *ZNF652*, *OCIAD1*, *C21orf58*,  
82 *IL11RA*) contributing to PC2 increased in expression 28 days post-vaccination in the 2012 and 2013  
83 seasons while decreasing in expression in the other seasons. This differential expression analysis shows  
84 that there are large variations in vaccine-induced transcriptional signatures between seasons which, in  
85 young adults, might be explained in part by vaccine composition.

86  
87 Given the substantial seasonal variation in the number of DEGs, we next performed an analysis of  
88 differential expression of gene modules using QuSAGE to quantify the gene module activity of 346  
89 previously defined BTMs (23). There were 262 differentially expressed modules (DEMs) (FDR  $< 0.05$ ; SI  
90 File 4, SI Appendix, Fig. S4A). Similar to the gene-level analysis, no significant changes were identified  
91 in the 2014 season, but six modules (*cell cycle and growth arrest (M31)*, *chemokines and inflammatory*  
92 *molecules in myeloid cells (M86.0)*, *enriched for TF motif TTCNRGNNNTTC*, *leukocyte differentiation*  
93 *(M160)*, *putative targets of PAX3 (M89.1)*, and *signaling in T cells (I) (M35.0)*) were significantly  
94 downregulated in young adults at D28 in four of five seasons (Fig. 2D). These changes were largely  
95 driven by decreases in *DUSP1/2*, *EGR1/2*, *JUN/JUNB*, *FOS/FOSB*, *TNF*, *CD83*, and *IL1B*. Thus, while  
96 there was substantial variability in the signatures induced by vaccination across multiple seasons, there is  
97 a shared signature consisting of three genes and six modules which was downregulated at D28 in four of  
98 five seasons.

99

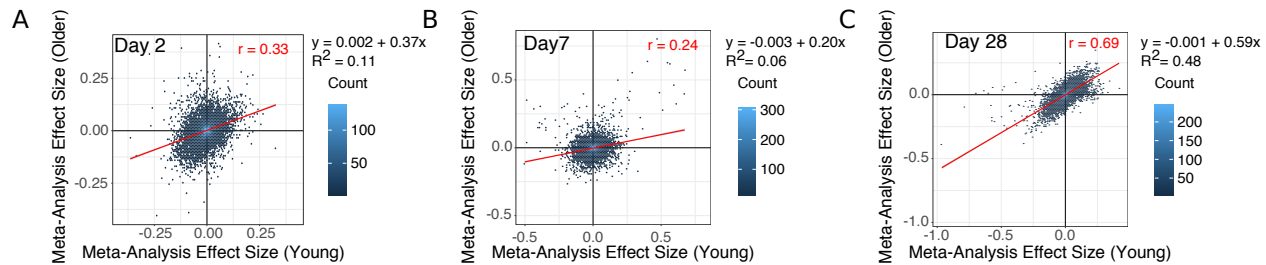


**Figure 3**

**Vaccine-Induced Changes are Correlated Between Young and Older Adults at Day 28.** Scatter plots show the meta-analysis effect sizes of changes post-vaccination for every gene in young vs older adults on days 2 (A), 7 (B) and 28 (C) post-vaccination.

### *Shared Vaccine-Induced Signatures Across Five Seasons*

The differential expression approach is limited by fixed fold change and significance cutoffs that may vary between seasons. To increase our power to identify shared signatures across seasons and in older adults, we performed a meta-analysis at the individual gene and gene module level. We identified 338 genes with significantly altered expression post-vaccination ( $FDR < 0.05$ ; *SI File 5*). In young adults, we identified significant genes at D2, D7 and D28 with little overlap among genes on each day. Genes induced on D2 were moderately enriched for innate immune genes from InnateDB (<http://innatedb.com/>) including *MYH9*, *TYK2*, *GLRX*, and *IP6K1* ( $p = 0.12$ , hypergeometric test). Some of the genes consistently induced at D7 included *IGLL1*, *CD38*, *ITM2C*, *TNFRSF17*, *MZB1*, and *TXNDC5*. We previously identified *TNFRSF17*, B cell maturation antigen, as induced seven days following influenza vaccination (26), and it was also identified as a predictive marker gene of antibody response to multiple vaccines including influenza, meningococcal conjugate (MCV4), and yellow fever (YF17D) vaccines (11, 23, 27–29). Consistent with the individual season analysis, the majority of genes identified by the meta-analysis were altered at D28; these D28 DEGs included *DUSP1*, *DUSP2*, and *CCL3L3*, identified in the single-season analysis, and many other downregulated genes including *IL1B*, *CCL3*, and *JAK1*. Thus, there are consistent changes identified across all seasons in young adults at every time point measured.

In older adults, we identified 125 genes with significantly altered expression at D28, but no genes with significantly altered expression at D2 or D7 (*SI File 5*). The most significantly increased gene at D28 is *XRNI*, the primary 5' to 3' cytoplasmic exonuclease involved in mRNA degradation (30). *XRNI* plays a critical role in the control of RNA stability in general, but in addition appears to regulate the response to viral infection at several levels—for example, by targeting viral RNAs for degradation (31), or regulating levels of potential activating ligands such as double-stranded RNA (32). Notably, *XRNI* has also been reported to facilitate replication of influenza and other viruses by inhibiting host gene expression (33, 34) - suggesting that dysregulated expression of *XRNI* in older adults could influence host response to vaccination. We identified 3 genes shared between both age groups: *ARRDC3* and *USP30* were downregulated while *TNPO1* was upregulated, all at D28. *ARRDC3* encodes a member of the arrestin protein family which regulates G protein-mediated signaling and is implicated in regulating metabolism (35). *USP30* is a ubiquitin-specific protease that acts as a mitochondrial deubiquitinating enzyme (36). *TNPO1* encodes Transportin-1 that serves to import proteins into the nucleus (37). The effect sizes of all genes at D28 were positively correlated between young and older adults with weak positive associations

138 at D2 and D7 (Fig. 3). These results provide additional evidence that transcriptional changes are broadly  
139 similar in young and older adults at D28 post-vaccine.

140  
141 We carried out a gene set level meta-analysis using QuSAGE to combine probability density estimates of  
142 gene module activity for each season (38). We identified 186 BTMs significantly altered post-vaccination  
143 across five seasons ( $FDR < 0.05$ ; *SI File 4*). The module with the largest increase in activity was *plasma*  
144 *cells, immunoglobulins (M156.1)* which peaked on D7 with a combined fold change of 1.17 in young  
145 adults and 1.08 in older adults at D7. Most BTMs showing significant changes were identified in young  
146 adults and, unlike the individual gene level, there was a large overlap between sets at each time point,  
147 suggesting the same module changes were sustained over the 28 days following vaccination (*SI Appendix*,  
148 Fig. S4A). Indeed, a heatmap of module activity shows that in young adults, transcriptional changes  
149 continued to intensify at D28 for many modules rather than returning to the baseline state (*SI Appendix*,  
150 Fig. S6). Older adults showed a qualitatively similar pattern to young adults on D2 and D28, but not D7.  
151 The majority (40/59) of the modules significantly altered in older adults on D28 were also significantly  
152 altered in young adults at D28 (*SI Appendix*, Fig. S4A). The modules downregulated on D28 in both  
153 young and older adults were annotated with antigen processing and presentation (M95.0, M95.1, M28,  
154 M71, M200, M5.0) and T cell activation (M36, M44, M52). The modules upregulated on D28 included  
155 *golgi membrane (II) (M237)*, *enriched in DNA interacting proteins (M182)*, and *chaperonin mediated*  
156 *protein folding (I, II) (M204.0, M204.1)*. Taken together, the high correlation between individual gene  
157 changes and overlap of many BTMs suggest a convergence toward a common transcriptional program in  
158 young and older adults at D28.

### 159 ***Age-Associated Genes are Induced 7 Days Post-Vaccination***

160  
161  
162 A meta-analysis across all five seasons revealed markedly different baseline transcriptional profiles in  
163 young vs. older adults, with 1,072 genes significantly altered ( $FDR < 0.05$ , *SI File 6*). Of these age-  
164 associated genes, 204 genes were also significantly induced by the vaccine in young adults and 125 genes  
165 in older adults. We tested whether age-associated genes were enriched for vaccine-induced genes at each  
166 time point and found that the overlap was significantly more than expected by chance for the 6 age-  
167 associated genes induced on D7 in young adults ( $p = 0.017$ , hypergeometric test). Of these 6 overlapping  
168 genes, 5 genes (*ITM2C*, *MZB1*, *IGLL1*, *TNFRSF17*, and *TXNDC5*) exhibited decreased basal expression  
169 in older adults while 1 (*SELENOS*) exhibited increased basal expression compared to young adults. While  
170 these genes were induced in young adults, they were not significantly induced in older adults on D7.  
171 Notably, *MZB1* and *TNFRSF17* are B cell associated genes, suggesting that older adults have decreased B  
172 cell activity pre-vaccination and fail to induce the same B cell response as young adults at D7. *SELENOS*  
173 encodes selenoprotein S, which is involved in degrading misfolded endoplasmic reticulum (ER) proteins  
174 and influences inflammation via the ER stress response (39, 40). Our results show that age-associated  
175 genes are significantly over-represented in the set of genes altered in young adults 7 days post-  
176 vaccination.

177  
178 We next performed a meta-analysis of BTMs between age groups at baseline and identified 120 modules  
179 significantly altered with age ( $FDR < 0.05$ , *SI File 7*). Most of the modules that were decreased with age  
180 were associated with adaptive immunity, whereas those that had increased expression with age were  
181 mostly innate and inflammatory modules (reflecting age-associated inflammatory dysregulation; *SI*

182 *Appendix*, Fig. S7B). Of these 120 modules, 52 were also significantly altered post-vaccination; however,  
183 the overlap at each time point was not significantly more than expected by chance (hypergeometric  $p >$   
184  $0.05$ , *SI Appendix*, Fig. S7A). Thus, age-related genes are enriched among the genes induced at D7 in  
185 young adults while no gene modules were significantly over-represented.

186

### 187 ***Post-Vaccination Predictors of Antibody Response***

188

189 We next asked whether any transcriptional changes post-vaccination could discriminate high antibody  
190 responders (HR) from low antibody responders (LR). Regularized logistic regression models with an L1  
191 (Lasso) or L1 and L2 (Elastic Net) penalties were fit to identify genes predictive of antibody response. In  
192 addition, to identify biologically interpretable predictors we used the Logistic Multiple Network-  
193 constrained Regression (LogMiNeR) framework (26) that facilitates the generation of predictive models  
194 with improved biological interpretability over standard methods. We combined the fold changes in gene  
195 expression data post-vaccination from five seasons and trained LogMiNeR to predict HR vs. LR in young  
196 and older cohorts separately (*SI Appendix*). At each time point, models were trained on all five seasons of  
197 data (except for D2, which was not available in the 2010 season; see *Methods*). Publicly-available data  
198 sets from independent groups were used to validate the models. For the models built from expression  
199 changes at D2 or D28, no studies at identical time-points were available, so we attempted to validate these  
200 models on studies with similar time points (day 1 or 3 in (11) and day 14 in (13)). While we could build  
201 predictive models on our data (median AUC  $\geq 0.75$ ) they did not validate on other data sets at the  
202 (different) time points available (median AUC  $\leq 0.55$ ).

203

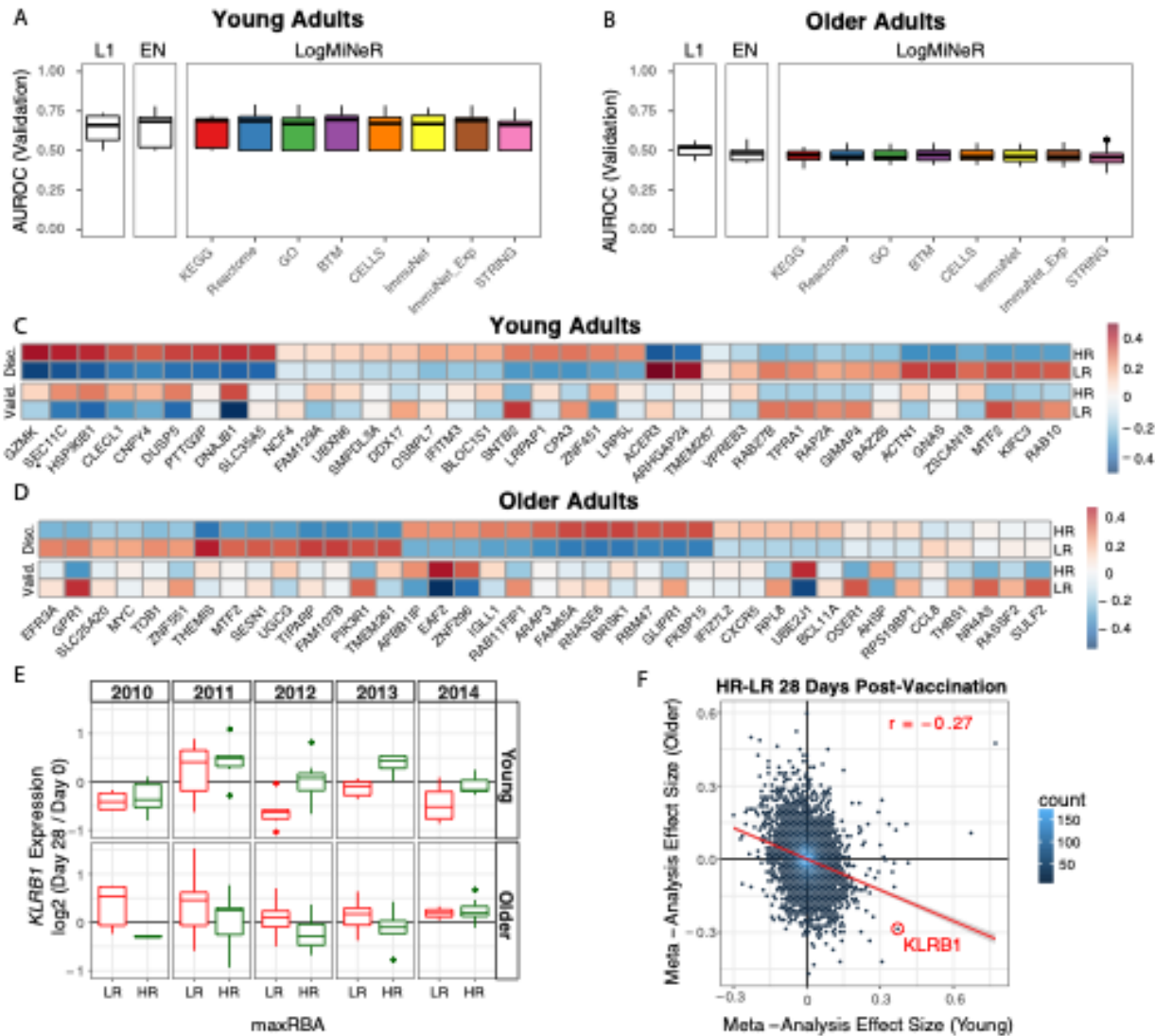
204 For D7 post-vaccine, direct validation data were available in independent datasets. In young adults, D7  
205 models were predictive for HR in the discovery and validation (11) datasets (Fig. 4A). Another MAP  
206 kinase phosphatase acting on ERK1/2, *DUSP5*, was one of 37 genes selected by the Lasso model whose  
207 expression was increased in HR (Fig. 4C). *DUSP5* is expressed in multiple immune cell types such as B  
208 cells (including plasma cells), T cells, dendritic cells, macrophages and eosinophils (41). In murine T  
209 cells, *DUSP5* appears to promote the development of short-lived effector CD8<sup>+</sup> T cells and inhibit  
210 memory precursor effector cell generation in an LCMV infection model (42); while optimizing memory  
211 precursor cell generation would be the goal of vaccination, the upregulation of *DUSP5* in HR could  
212 reflect regulation of the balance between short-lived vs. memory precursor effector CD8<sup>+</sup> T cells. A  
213 sensitivity analysis of the maxRBA cutoff shows that the average expression of predictive genes is  
214 consistent across a range of definitions for HR and LR (20<sup>th</sup> – 40<sup>th</sup> percentile; *SI Appendix*, Fig. S2C-D).  
215 Using LogMiNeR, the models were consistently enriched for the *B Cell* signature as well as the KEGG  
216 *chemokine signaling pathway* (*SI File 8*).

217

218 In older adults, models predicting antibody responses built from D7 gene expression were highly  
219 predictive in the discovery dataset but did not validate on an independent dataset (13) (Fig. 4B, D).  
220 Expression of the Solute Carrier Family 25 gene *SLC25A20* of mitochondrial transporters contribute to  
221 predicting HR vs. LR in older adults. *SLC25A20* is the carrier for carnitine and acylcarnitine (43), and so  
222 would be expected to be crucial for the transport of fatty acids into mitochondria. The models of response  
223 in older adults were significantly enriched for several BTMs of monocyte signatures as well as *TLR and*  
224 *Inflammatory Signaling (M16)*, which positively predicted vaccine response; together with previous  
225 studies linking age-associated impairments in TLR function to influenza vaccine antibody response (44,

226 45), these findings provide additional support for the crucial role of innate immune function in  
227 vaccination (*SI File 8*).

228  
229 Notably, none of the models built in young adults at any time point are predictive in older adults ( $AUC \leq$   
230 0.5). In fact, models built on transcriptional changes at D28 in young adults had a median AUC near 0.8  
231 in young adults, but no more than 0.3 in older adults, suggesting that the same genes predictive of HR in  
232 young adults predicted LR in older adults (*SI Appendix*; [Fig. S8E](#)). The Lasso models making these  
233 predictions often chose a single gene, Killer Cell Lectin Like Receptor B1 (*KLRB1*, also known as  
234 *CD161*), which was driving this inverse pattern ([Fig. 4E](#)). *KLRB1* is an inhibitory receptor on NK cells  
235 (46, 47) and is also a biomarker of Th17 cells (48–50). Notably, changes in *KLRB1* expression in sorted  
236 CD4 and CD8 T cells at D28 closely mirrored the changes in PBMCs for young, but not older adults (*SI*  
237 *Appendix*, [Fig. S8A-B](#)). We confirmed this inverse correlation between age groups on a genome-wide  
238 scale by performing a meta-analysis comparing HR vs. LR (*SI File 9*). We observed a weak negative  
239 correlation in effect sizes between young and older adults at D28 ( $r = -0.27$ ; [Fig. 4F](#)). We confirmed this  
240 negative correlation in effect sizes between young and older adults using a virus neutralization assay  
241 (VNA) in a test sample of blood from seasons 2011 and 2012 ( $r = -0.32$ ; *SI Appendix*, [Fig. S8D](#)). Thus,  
242 expression changes of many genes at D28 have opposing signs between age groups for the effect size  
243 comparing HR vs. LR, and a single gene, *KLRB1*, predicts response with  $AUC > 0.7$  in opposing  
244 directions in young vs. older adults.



245

246 **Figure 4**

247 **Post-Vaccination Transcriptional Predictors of Antibody Response.** (A and B) Boxplots of the area  
 248 under the receiver operating characteristic curve (AUROC) in the validation data for Lasso (L1), Elastic  
 249 Net (EN), and Logistic Multiple Network-constrained Regression (LogMiNeR) models built from day 7  
 250 transcriptional changes in young (A) and older (B) adults. 50 iterations of cross-validation were  
 251 performed. x-labels indicate the prior knowledge network for LogMiNeR (see *SI Appendix*). (C and D)  
 252 Heatmaps of Discovery (Disc.) and Validation (Valid.) data showing the z-score of the fold change for  
 253 individual genes selected by the L1 models in any iteration for young (C) and older (D) adults. (E)  
 254 Boxplots of *KLRB1* expression changes in PBMCs 28 days post-vaccination in low responders (LR) and  
 255 high responders (HR). (F) A scatter plot of the gene effect sizes comparing HR to LR 28 days post-  
 256 vaccination in young vs older adults. *KLRB1* is indicated as a gene that has a positive effect size in one  
 257 age group and negative effect size in the other.

258

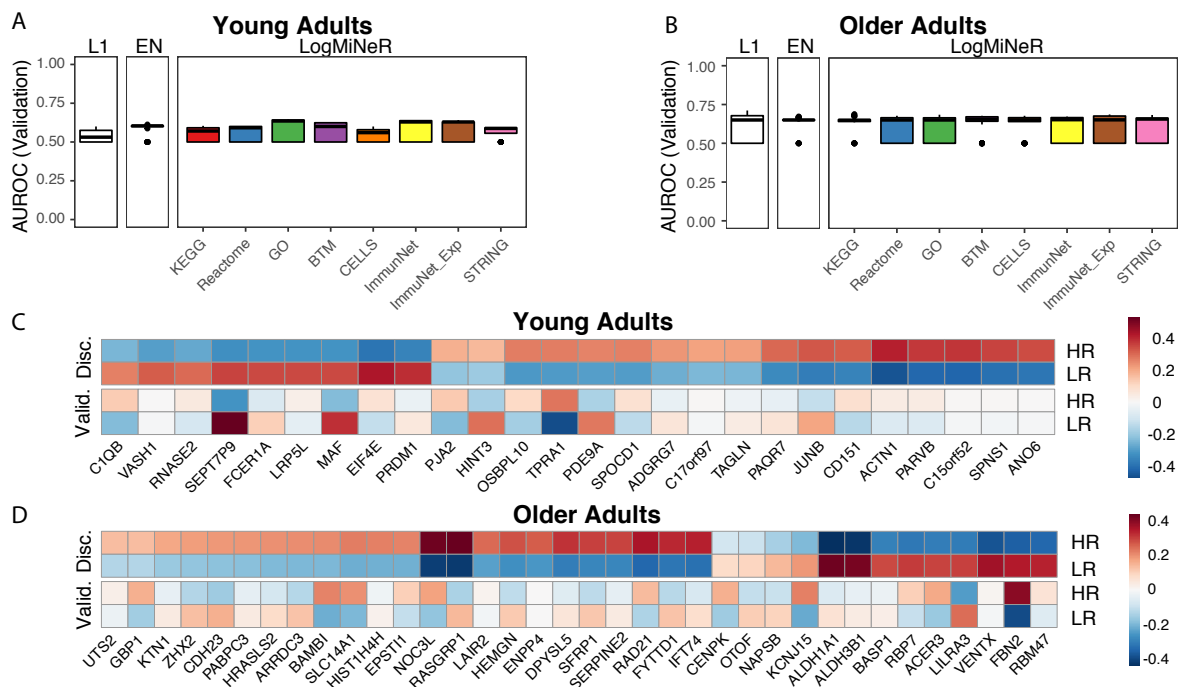
259

260

## 261 *Baseline Predictors of Antibody Response*

262

263 We next sought to identify baseline transcriptional predictors of antibody response. In young adults,  
 264 LogMiNeR models were predictive above random on discovery and validation (11) (Fig. 5A) datasets.  
 265 Lasso models included the gene *VASH1*, known as an angiogenesis inhibitor and mediator of stress  
 266 resistance in endothelial cells, which was expressed at lower levels in HRs (Fig. 5C); notably, the KEGG  
 267 gene set *leukocyte transendothelial migration* was significantly enriched in over 50% of the models when  
 268 LogMiNeR was used with ImmuneNet as prior knowledge (51). Another predictive gene, *EIF4E*, a  
 269 translation initiation factor important in type I interferon production, was decreased in HRs. A sensitivity  
 270 analysis of the maxRBA cutoff shows that the average expression of predictive genes is consistent across  
 271 a range of definitions for HR and LR (20<sup>th</sup> – 40<sup>th</sup> percentile; SI Appendix, Fig. S2E-F). Finally, the BTMs  
 272 *cell adhesion (M51)* and *B cell surface signature (S2)* were consistently enriched in the models (SI File  
 273 8). In older adults, LogMiNeR models were also predictive on the discovery and one validation dataset  
 274 (9) (Fig. 5B) but not another (13) (SI Appendix, Fig. S8C). Two of the individual genes that predict  
 275 response, *ALDH1A1* and *ALDH3B1*, are aldehyde dehydrogenases which metabolize vitamin A to retinoic  
 276 acid (Fig. 5D). Recently, aldehyde dehydrogenases were implicated in antiviral innate immunity as  
 277 mediators of the interferon response through their role in the biogenesis of retinoic acid (52). Multiple  
 278 monocyte gene sets are enriched in the predictive genes, including the BTM *enriched in monocytes (II)*  
 279 (*M11.0*), which negatively predicts vaccine response (SI File 8). Thus, these baseline predictive models  
 280 built from five seasons of transcriptional profiling data provide further evidence for functional  
 281 distinctions present in subjects prior to vaccination that influence the immunologic response to influenza  
 282 vaccine in young and older adults.  
 283



284

## 285 **Figure 5**

286 **Baseline Transcriptional Predictors of Antibody Response.** (A and B) Boxplots of the area under the  
 287 receiver operating characteristic curve (AUROC) in the validation data for Lasso (L1), Elastic Net (EN),



288 and Logistic Multiple Network-constrained Regression (LogMiNeR) models built from baseline (pre-  
289 vaccination) transcriptional profiles in young (A) and older (B) adults (9). 50 iterations of cross-validation  
290 were performed. x-labels indicate the prior knowledge network for LogMiNeR (see *SI Appendix*). (C and  
291 D) Heatmaps of Discovery (Disc.) and Validation (Valid.) data showing the z-score of the fold change for  
292 individual genes selected by the L1 models in any iteration for young (C) and older (D) adults.

293  
294

### 295 ***Behavior of Published Signatures Over Five Seasons***

296

297 To link our findings to previously identified influenza vaccine signatures, we performed a comprehensive  
298 assessment of the behavior of 1,603 previously published individual gene and gene module signatures in  
299 our data set. We manually curated published signatures from studies that carried out transcriptional  
300 profiling on adult cohorts after influenza vaccination (9, 11, 13, 15, 27, 53). We further limited the  
301 signatures to shared time points post-vaccination. This set of findings describe 935 response-associated  
302 and 653 temporal signatures in B cells and PBMCs as well as 15 age-associated signatures (*SI File 10*).

303

304 Most of the previously published signatures we validated in our data were single genes induced 7 days  
305 post-vaccination in PBMCs or B cells (*SI Appendix*, Fig. S9). Of the 135 signatures that showed  
306 significant differential expression ( $p < 0.001$ ), 103 changed in the same direction as the published  
307 signature. In PBMCs we validated 26 D7 vaccine-induced genes including four genes independently  
308 discovered in our meta-analysis: *CD38*, *ITM2C*, *TNFRSF17*, and *SPATS2* (*SI Appendix*, Fig. S9B) (11).  
309 *CD38* is upregulated on the surface of antibody secreting cells, and *TNFRSF17*, or B cell maturation  
310 antigen (*BCMA*) is a receptor for B cell activating factor (*BAFF*) expressed on memory B cells and  
311 plasma cells (54). Notably, validated vaccine-induced genes in B cells include several associated with  
312 mitochondrial function whose expression was upregulated at Day 7, including *UQCRCQ* (ubiquinol  
313 cytochrome c reductase, complex III, subunit VII), *ME2* (NAD-dependent malic enzyme), *TAL*  
314 (transaldolase 1), and *GLDC* (glycine decarboxylase) (*SI Appendix*, Fig. S9A). We validated several  
315 modules significantly associated with antibody response at baseline in young and older adults (*SI*  
316 *Appendix*, Fig. S9D) (13). Of these modules, one positively associated with antibody response (*enriched*  
317 *in B cells (I) (M47.0)*) is enriched in our baseline predictive model of young adults and three negatively  
318 associated with antibody response are enriched in our baseline predictive model of older adults (*Monocyte*  
319 *surface signature (S4)*, *myeloid cell enriched receptors and transporters (M4.3)*, *enriched in monocytes*  
320 *(II) (M11.0)*). Interestingly, these latter three modules are also enriched in predictive models of HR vs LR  
321 from D7 fold changes. Finally, there are seven validated single genes whose fold change at D7 is  
322 positively associated with antibody response in young adults (*SI Appendix*, Fig. S9C) (11). One of these  
323 genes, *HSP90B1*, or *gp96* – an ER-based chaperone protein implicated in innate and adaptive immune  
324 function – is also selected as a predictive gene of antibody response (55, 56).

325

## 326 **Discussion**

327

328 This study is the first to evaluate the transcriptomic response to influenza vaccination in young and older  
329 adults in five consecutive vaccine seasons with three different vaccine compositions. We sought to  
330 address whether common signatures of vaccine response or transcriptional predictors of antibody  
331 response could be elucidated despite differences in seasonal vaccine composition.

332  
333 To adjust for the inverse relationship between baseline antibody titers and vaccine-induced antibody  
334 production, we developed a novel vaccine response endpoint, maxRBA, to automatically correct for  
335 variation in baseline titers; this allowed us to demonstrate an age-associated decrease in antibody response  
336 in gender-matched participants. Comparing the transcriptional profiles across five seasons revealed  
337 substantial seasonal variability in both the magnitude as well as direction of response. For example, the  
338 vaccines administered in the 2010 and 2011 seasons elicited large changes in gene expression, but no  
339 statistically significant DEGs were found in the 2014 season despite a comparable sample size.  
340 Potentially, the large transcriptional changes observed in 2010 and 2011 could reflect the introduction of  
341 the A/California/7/2009 viral pandemic strain to the seasonal vaccine (as well as a change in the H3N2  
342 vaccine strain beginning in 2010—the only year of the five studied when both influenza A strains  
343 changed). Notably, a principal component analysis revealed similar vaccine-induced signatures in the  
344 2011 and 2014 seasons and in the 2012 and 2013 seasons. The similarities between the 2011 and 2014  
345 seasons are intriguing because in both seasons the composition of the vaccine was identical to that in the  
346 preceding year, perhaps suggesting that these gene signatures reflect a relatively recent recall response. In  
347 contrast, the 2012 and 2013 vaccines each contained two strains which had not been present in the  
348 previous year's vaccine. We did not observe the same trends in older adults; nonetheless, our results  
349 indicate that changes in vaccine composition, influencing factors such as vaccine strain immunogenicity  
350 and the effects of previous vaccination or infection, can alter the transcriptional response to influenza  
351 immunization.

352  
353 Despite substantial inter-season variability, we identified shared vaccine-induced signatures in both young  
354 and older adults at D28. We expected D28 expression profiles to be similar to baseline; however, there  
355 were numerous transcriptional changes at D28 that were consistent across seasons with different vaccine  
356 compositions. Some of the most significant changes identified from single-season differential expression  
357 analysis in four out of five seasons were in *DUSP1*, *DUSP2*, and *CCL3L3*; moreover, *DUSP2* expression  
358 was also decreased in sorted CD4+ and CD8+ T cells from both young and older adults at D28. It is  
359 notable that a basal age-related alteration in phosphorylation of *DUSP1*, a negative regulator of IL-10  
360 production, was associated with increased expression of IL-10 in monocytes from older adults (seen pre-  
361 and post-influenza vaccination) (57) and that increased *DUSP6* expression was associated with impaired  
362 T cell receptor signaling in CD4+ T cells from older adults (58). These results emphasize the importance  
363 of modulation of MAP kinase function, such as through phosphatases of the DUSP family, in the  
364 regulation of influenza vaccine response. Surprisingly, early response signatures at D2 and D7 post-  
365 vaccination were not as consistent across seasons as D28 signatures in a meta-analysis of genes and gene  
366 modules. One potential hypothesis that explains this observation is that temporal variations in early  
367 responses across seasons were not captured at the time points used, and that responses at D28 are less  
368 variable, and thus were captured in every season. It is possible that this common transcriptional program  
369 at D28 reflects a convergence towards resolution of the vaccine response in both young and older adults.  
370 However, a substantial number of BTMs showed upregulated activity at D28 without evidence of  
371 resolution to baseline, particularly in young adults; notably, we previously found evidence of enhanced  
372 TNF-alpha and IL-6 production in monocytes 28 days post-influenza immunization (57) that was blunted  
373 in monocytes from older adults. Thus, it remains possible that the transcriptional signature we observed  
374 also reflects elements of an ongoing immune activated state several weeks after vaccination.  
375

376 We built predictive models of antibody response from post-vaccination transcriptional responses which  
377 were successfully validated in an independent cohort of young adults. Although transcriptional changes  
378 were correlated between age groups at D28, models of antibody response built in young adults did not  
379 validate in older adults. Strikingly, we identified a genome-wide inverse correlation between the effect  
380 size of genes discriminating HR and LR at D28 and confirmed this finding with both HAI and VNA  
381 titers. A similar inverse correlation related to age was recently reported using baseline (D0) gene  
382 expression signatures (15). We identified a single gene, *KLRB1*, whose expression alone predicted  
383 response in both age groups but in opposite directions. In young adults, changes in *KLRB1* expression  
384 were also observed in sorted CD4 and CD8 T cells, perhaps reflecting the finding that *KLRB1* expression  
385 is increased in populations of memory T cells (59). Furthermore, *KLRB1*<sup>hi</sup> CD8<sup>+</sup> T cells are self-renewing  
386 memory cells that are able to reconstitute the memory T cell pool after chemotherapy (60). Thus, *KLRB1*  
387 induction in young adults may reflect an increase in memory T cell populations. In older adults, these  
388 expression patterns were not observed in sorted T cells, implying that *KLRB1* expression in another cell  
389 type, perhaps NK cells or Th17 cells, was the basis for the predictive performance.

390  
391 We also built and validated predictive models of antibody response in young and older adults from D0  
392 gene expression data. One of the predictive genes in young adults, *VASH1*, showed evidence of genetic  
393 regulation of gene expression in a previous study of influenza vaccination, suggesting that genotype may  
394 have predictive power to explain the antibody response (8). Leukocyte migration and a B cell surface  
395 signature were enriched in the predictive models. This is consistent with a recently reported meta-analysis  
396 which included baseline transcriptional profiles from the 2010, 2011, and 2012 seasons of the present  
397 study and validated a temporally stable B cell receptor signaling gene module that positively predicted  
398 response at baseline (15). While the *B cell surface signature (S2)* module we identified was not the same  
399 one identified in the previous study, our findings further support the implication of B cell transcriptional  
400 signatures as pre-vaccine biomarkers of antibody response in young adults. In older adults, we  
401 incorporated prior knowledge on gene coexpression using LogMiNeR to identify monocyte signatures  
402 which were enriched in the predictive models and were negatively associated with antibody response. Our  
403 model validated on one older adult cohort (9) but not another (13); this may reflect substantial variability  
404 in cohorts of older adults, which would be expected to be more heterogeneous in terms of comorbid  
405 medical conditions or medication use compared to young adults. Finally, we linked our findings to  
406 previously identified influenza vaccination signatures by performing a comprehensive assessment of  
407 1,603 previously published individual gene and gene module signatures. We present the signatures that  
408 validate in any season or a meta-analysis of all seasons of our data to highlight the most consistent set of  
409 genes and gene modules associated with vaccination or antibody response in PBMC and B cells.

410  
411 In summary, we profiled nearly 300 young and older adults across five vaccination seasons and, despite  
412 substantial seasonal variability in vaccine-induced transcriptional signatures, identified a core  
413 transcriptional signature shared between seasons and across age groups 28 days post-vaccination. In  
414 addition, we defined a new endpoint (maxRBA) to capture antibody response relative to baseline titer and  
415 were able to predict response in young and older adults separately using baseline transcriptional profiles.  
416 Our results suggest that vaccine composition, in concert with differences in pre-existing immunity and  
417 other individual factors, dramatically influences immune response to inactivated influenza vaccination.  
418 Furthermore, this work is a step toward understanding the underlying mechanisms of response in older  
419 adults which may be beneficial for rationally designing more effective vaccines.

420

## 421 **Acknowledgments**

422

423 We gratefully acknowledge Dr. Randy Albrecht and Dr. Adolfo Garcia-Sastre at the Icahn School of  
424 Medicine at Mount Sinai, who led the Human Immunology Project Consortium (HIPC) core for influenza  
425 viral neutralization assays. This work was supported by NIH grant U19 AI089992, K24 AG042489, and  
426 by the Claude D. Pepper Older Americans Independence Center at Yale (to H.J.Z. and A.C.S.: P30  
427 AG021342). Computational resources and support were provided by the Yale Center for Research  
428 Computing [NIH grants RR19895 and RR029676-01]. H.J.Z. was supported by a GEMSSTAR award  
429 from NIA (R03 AG050947). D.G.C. was supported by NIH training grant T32 EB019941. S.A. was  
430 supported by the NSF Graduate Research Fellowship Program [grant number DGE-1122492]. Any  
431 opinions, findings and conclusions or recommendations expressed in this material are those of the authors  
432 and do not necessarily reflect the views of the National Science Foundation.

433

## 434 **Author Contributions**

435 Conceptualization, S.M.K., A.C.S., and S.H.K.; Software, S.A.; Formal Analysis, S.A., D.G.C., and  
436 H.M.; Investigation, S.M., H.J.Z., T.B., I.U., K.P., T.P.B, and R.B.B.; Data Curation, S.T. and H.M.;  
437 Writing – Original Draft, S.A., A.C.S., and S.H.K.; Writing – Review & Editing, All Authors;  
438 Visualization, S.A., D.G.C.

439

## 440 **References**

441

- 442 1. Ohmit, S. E., J. C. Victor, E. R. Teich, R. K. Truscon, J. R. Rotthoff, D. W. Newton, S. a Campbell, M.  
443 L. Boulton, and A. S. Monto. 2008. Prevention of symptomatic seasonal influenza in 2005-2006 by  
444 inactivated and live attenuated vaccines. *J. Infect. Dis.* 198: 312–317.
- 445 2. Frey, S., T. Vesikari, A. Szymczakiewicz-Multanowska, M. Lattanzi, A. Izu, N. Groth, and S. Holmes.  
446 2010. Clinical Efficacy of Cell Culture-Derived and Egg-Derived Inactivated Subunit Influenza Vaccines  
447 in Healthy Adults. *Clin. Infect. Dis.* 51: 997–1004.
- 448 3. Jackson, L. a, M. J. Gaglani, H. L. Keyserling, J. Balser, N. Bouveret, L. Fries, and J. J. Treanor. 2010.  
449 Safety, efficacy, and immunogenicity of an inactivated influenza vaccine in healthy adults: a randomized,  
450 placebo-controlled trial over two influenza seasons. *BMC Infect. Dis.* 10: 71.
- 451 4. Monto, A. S., S. E. Ohmit, J. G. Petrie, E. Johnson, R. Truscon, E. Teich, J. Rotthoff, M. Boulton, and  
452 J. C. Victor. 2009. Comparative efficacy of inactivated and live attenuated influenza vaccines. *N. Engl. J.*  
453 *Med.* 361: 1260–1267.
- 454 5. Beran, J., V. Wertzova, K. Honegr, E. Kaliskova, M. Havlickova, J. Havlik, H. Jirincova, P. Van Belle,  
455 V. Jain, B. Innis, and J.-M. Devaster. 2009. Challenge of conducting a placebo-controlled randomized  
456 efficacy study for influenza vaccine in a season with low attack rate and a mismatched vaccine B strain: a  
457 concrete example. *BMC Infect. Dis.* 9: 2.
- 458 6. Goodwin, K., C. Viboud, and L. Simonsen. 2006. Antibody response to influenza vaccination in the  
459 elderly: A quantitative review. *Vaccine* 24: 1159–1169.
- 460 7. Bucasas, K. L., L. M. Franco, C. a Shaw, M. S. Bray, J. M. Wells, D. Niño, N. Arden, J. M. Quarles, R.  
461 B. Couch, and J. W. Belmont. 2011. Early patterns of gene expression correlate with the humoral immune  
462 response to influenza vaccination in humans. *J. Infect. Dis.* 203: 921–9.
- 463 8. Franco, L. M., K. L. Bucasas, J. M. Wells, D. Niño, X. Wang, G. E. Zapata, N. Arden, A. Renwick, P.  
464 Yu, J. M. Quarles, M. S. Bray, R. B. Couch, J. W. Belmont, and C. a Shaw. 2013. Integrative genomic

- 465 analysis of the human immune response to influenza vaccination. *Elife* 2: e00299.
- 466 9. Furman, D., V. Jovic, B. Kidd, S. Shen-Orr, J. Price, J. Jarrell, T. Tse, H. Huang, P. Lund, H. T.
- 467 Maecker, P. J. Utz, C. L. Dekker, D. Koller, and M. M. Davis. 2013. Apoptosis and other immune
- 468 biomarkers predict influenza vaccine responsiveness. *Mol. Syst. Biol.* 9: 659.
- 469 10. Tan, Y., P. Tamayo, H. Nakaya, B. Pulendran, J. P. Mesirov, and W. N. Haining. 2014. Gene
- 470 signatures related to B-cell proliferation predict influenza vaccine-induced antibody response. *Eur. J.*
- 471 *Immunol.* 44: 285–295.
- 472 11. Tsang, J. S., P. L. Schwartzberg, Y. Kotliarov, A. Biancotto, Z. Xie, R. N. Germain, E. Wang, M. J.
- 473 Olnes, M. Narayanan, H. Golding, S. Moir, H. B. Dickler, S. Perl, and F. Cheung. 2014. Global analyses
- 474 of human immune variation reveal baseline predictors of postvaccination responses. *Cell* 157: 499–513.
- 475 12. Obermoser, G., S. Presnell, K. Domico, H. Xu, Y. Wang, E. Anguiano, L. Thompson-Snipes, R.
- 476 Ranganathan, B. Zeitner, A. Bjork, D. Anderson, C. Speake, E. Ruchaud, J. Skinner, L. Alsina, M.
- 477 Sharma, H. Dutartre, A. Cepika, E. Israelsson, P. Nguyen, Q. A. Nguyen, a. C. Harrod, S. M. Zurawski,
- 478 V. Pascual, H. Ueno, G. T. Nepom, C. Quinn, D. Blankenship, K. Palucka, J. Banchereau, and D.
- 479 Chaussabel. 2013. Systems scale interactive exploration reveals quantitative and qualitative differences in
- 480 response to influenza and pneumococcal vaccines. *Immunity* 38: 831–844.
- 481 13. Nakaya, H. I., T. Hagan, S. S. Duraisingham, E. K. Lee, M. Kwissa, N. Rouphael, D. Frasca, M.
- 482 Gersten, A. K. Mehta, R. Gaujoux, G. M. Li, S. Gupta, R. Ahmed, M. J. Mulligan, S. Shen-Orr, B. B.
- 483 Blomberg, S. Subramaniam, and B. Pulendran. 2015. Systems Analysis of Immunity to Influenza
- 484 Vaccination across Multiple Years and in Diverse Populations Reveals Shared Molecular Signatures.
- 485 *Immunity* 43: 1186–1198.
- 486 14. Thakar, J., S. Mohanty, A. P. West, S. R. Joshi, I. Ueda, J. Wilson, H. Meng, T. P. Blevins, S. Tsang,
- 487 M. Trentalange, B. Siconolfi, K. Park, T. M. Gill, R. B. Belshe, S. M. Kaech, G. S. Shadel, S. H.
- 488 Kleinstein, and A. C. Shaw. 2015. Aging-dependent alterations in gene expression and a mitochondrial
- 489 signature of responsiveness to human influenza vaccination. *Aging (Albany, NY)*. 7: 38–52.
- 490 15. HIPC-CHI Signatures Project Team, T., and T. HIPC-I Consortium. 2017. Multicohort analysis
- 491 reveals baseline transcriptional predictors of influenza vaccination responses. *Sci. Immunol.* 2: eaal4656.
- 492 16. Song, J. Y., H. J. Cheong, I. S. Hwang, W. S. Choi, Y. M. Jo, D. W. Park, G. J. Cho, T. G. Hwang,
- 493 and W. J. Kim. 2010. Long-term immunogenicity of influenza vaccine among the elderly: Risk factors for
- 494 poor immune response and persistence. *Vaccine* 28: 3929–3935.
- 495 17. Yaari, G., C. R. Bolen, J. Thakar, and S. H. Kleinstein. 2013. Quantitative set analysis for gene
- 496 expression: A method to quantify gene set differential expression including gene-gene correlations.
- 497 *Nucleic Acids Res.* 41: e170.
- 498 18. Proost, P., P. Menten, S. Struyf, E. Schutyser, I. De Meester, and J. Van Damme. 2000. Cleavage by
- 499 CD26 / dipeptidyl peptidase IV converts the chemokine LD78 $\beta$  into a most efficient monocyte attractant
- 500 and CCR1 agonist. *Blood* 96: 1674–1680.
- 501 19. Kwak, S. P., D. J. Hakes, K. J. Martell, and J. E. Dixon. 1994. Isolation and Characterization of a
- 502 Human Dual Specificity Protein-Tyrosine Phosphatase Gene. *J. Biol. Chem.* 269: 3596–3604.
- 503 20. Rohan, P. J., P. Davis, C. A. Moskaluk, M. Kearns, P. J. Rohan, P. Davis, C. A. Moskaluk, M.
- 504 Kearns, H. Krutzsch, U. Siebenlist, and K. Kelly. 1993. PAC-1 : A Mitogen-Induced Nuclear Protein
- 505 Tyrosine Phosphatase. *Science (80-. )*. 259: 1763–1766.
- 506 21. Wei, W., Y. Jiao, A. Postlethwaite, J. M. Stuart, Y. Wang, D. Sun, and W. Gu. 2013. Dual-specificity
- 507 phosphatases 2: surprising positive effect at the molecular level and a potential biomarker of diseases.
- 508 *Genes Immun.* 14: 1–6.
- 509 22. Mohanty, S., S. R. Joshi, I. Ueda, J. Wilson, T. P. Blevins, B. Siconolfi, H. Meng, L. Devine, K.
- 510 Raddassi, S. Tsang, R. B. Belshe, D. A. Hafler, S. M. Kaech, S. H. Kleinstein, M. Trentalange, H. G.
- 511 Allore, and A. C. Shaw. 2015. Prolonged proinflammatory cytokine production in monocytes modulated
- 512 by interleukin 10 after influenza vaccination in older adults. *J. Infect. Dis.* 211: 1174–1184.
- 513 23. Li, S., N. Rouphael, S. Duraisingham, S. Romero-Steiner, S. Presnell, C. Davis, D. S. Schmidt, S. E.
- 514 Johnson, A. Milton, G. Rajam, S. Kasturi, G. M. Carlone, C. Quinn, D. Chaussabel, a K. Palucka, M. J.
- 515 Mulligan, R. Ahmed, D. S. Stephens, H. I. Nakaya, and B. Pulendran. 2014. Molecular signatures of

- 516 antibody responses derived from a systems biology study of five human vaccines. *Nat. Immunol.* 15: 195–  
517 204.
- 518 24. Kanehisa, M., and S. Goto. 2000. KEGG: Kyoto encyclopedia of genes and genomes. *Nucleic Acids*  
519 *Res.* 28: 27–30.
- 520 25. Abbas, a R., D. Baldwin, Y. Ma, W. Ouyang, A. Gurney, F. Martin, S. Fong, M. van Lookeren  
521 Campagne, P. Godowski, P. M. Williams, a C. Chan, and H. F. Clark. 2005. Immune response in silico  
522 (IRIS): immune-specific genes identified from a compendium of microarray expression data. *Genes*  
523 *Immun.* 6: 319–331.
- 524 26. Avey, S., S. Mohanty, J. Wilson, H. Zapata, S. R. Joshi, B. Siconolfi, S. Tsang, A. C. Shaw, and S. H.  
525 Kleinstein. 2017. Multiple network-constrained regressions expand insights into influenza vaccination  
526 responses. *Bioinformatics* 33: i208–i216.
- 527 27. Nakaya, H. I., J. Wrammert, E. K. Lee, L. Racioppi, S. Marie-Kunze, W. N. Haining, A. R. Means, S.  
528 P. Kasturi, N. Khan, G.-M. Li, M. McCausland, V. Kanchan, K. E. Kokko, S. Li, R. Elbein, A. K. Mehta,  
529 A. Aderem, K. Subbarao, R. Ahmed, and B. Pulendran. 2011. Systems biology of vaccination for  
530 seasonal influenza in humans. *Nat. Immunol.* 12: 786–795.
- 531 28. Gaucher, D., R. Therrien, N. Kettaf, B. R. Angermann, G. Boucher, A. Filali-Mouhim, J. M. Moser,  
532 R. S. Mehta, D. R. Drake, E. Castro, R. Akondy, A. Rinfret, B. Yassine-Diab, E. a Said, Y. Chouikh, M.  
533 J. Cameron, R. Clum, D. Kelvin, R. Somogyi, L. D. Greller, R. S. Balderas, P. Wilkinson, G. Pantaleo, J.  
534 Tartaglia, E. K. Haddad, and R.-P. Sékaly. 2008. Yellow fever vaccine induces integrated multilineage  
535 and polyfunctional immune responses. *J. Exp. Med.* 205: 3119–3131.
- 536 29. Querec, T. D., R. S. Akondy, E. K. Lee, W. Cao, H. I. Nakaya, D. Teuwen, A. Pirani, K. Gernert, J.  
537 Deng, B. Marzolf, K. Kennedy, H. Wu, S. Bennouna, H. Oluoch, J. Miller, R. Z. Vencio, M. Mulligan, A.  
538 Aderem, R. Ahmed, and B. Pulendran. 2009. Systems biology approach predicts immunogenicity of the  
539 yellow fever vaccine in humans. *Nat. Immunol.* 10: 116–125.
- 540 30. Mitchell, P., and D. Tollervey. 2000. mRNA stability in eukaryotes. *Curr. Opin. Genet. Dev.* 10: 193–  
541 198.
- 542 31. Molleston, J. M., and S. Cherry. 2017. Attacked from all sides: RNA decay in antiviral defense.  
543 *Viruses* 9.
- 544 32. Liu, S. W., G. C. Katsafanas, R. Liu, L. S. Wyatt, and B. Moss. 2015. Poxvirus decapping enzymes  
545 enhance virulence by preventing the accumulation of dsRNA and the induction of innate antiviral  
546 responses. *Cell Host Microbe* 17: 320–331.
- 547 33. Khapersky, D. A., S. Schmaling, J. Larkins-Ford, C. McCormick, and M. M. Gaglia. 2016. Selective  
548 Degradation of Host RNA Polymerase II Transcripts by Influenza A Virus PA-X Host Shutoff Protein.  
549 *PLoS Pathog.* 12: 1–25.
- 550 34. Gaglia, M. M., S. Covarrubias, W. Wong, and B. A. Glaunsinger. 2012. A common strategy for host  
551 RNA degradation by divergent viruses. *J Virol* 86: 9527–9530.
- 552 35. Patwari, P., and R. T. Lee. 2012. An expanded family of arrestins regulate metabolism. *Trends*  
553 *Endocrinol. Metab.* 23: 216–222.
- 554 36. Nakamura, N., and S. Hirose. 2008. Regulation of Mitochondrial Morphology by USP30, a  
555 Deubiquitinating Enzyme Present in the Mitochondrial Outer Membrane. *Mol. Biol. Cell* 19: 1903–1911.
- 556 37. Twyffels, L., C. Gueydan, and V. Krusys. 2014. Transportin-1 and Transportin-2: Protein nuclear  
557 import and beyond. *FEBS Lett.* 588: 1857–1868.
- 558 38. Meng, H., G. Yaari, C. R. Bolen, S. Avey, and S. H. Kleinstein. 2019. Gene set meta-analysis with  
559 Quantitative Set Analysis for Gene Expression (QuSAGE). *PLOS Comput. Biol.* 15: e1006899.
- 560 39. Curran, J. E., J. B. M. Jowett, K. S. Elliott, Y. Gao, K. Gluschenko, J. Wang, D. M. Abel Azim, G.  
561 Cai, M. C. Mahaney, A. G. Comuzzie, T. D. Dyer, K. R. Walder, P. Zimmet, J. W. MacCluer, G. R.  
562 Collier, A. H. Kissebah, and J. Blangero. 2005. Genetic variation in selenoprotein S influences  
563 inflammatory response. *Nat. Genet.* 37: 1234–1241.
- 564 40. Ye, Y., Y. Shibata, C. Yun, D. Ron, and T. A. Rapoport. 2004. A membrane protein complex  
565 mediates retro-translocation from the ER lumen into the cytosol. *Nature* 429: 841–847.
- 566 41. Jeffrey, K. L., M. Camps, C. Rommel, and C. R. Mackay. 2007. Targeting dual-specificity

- 567 phosphatases: manipulating MAP kinase signalling and immune responses. *Nat. Rev. Drug Discov.* 6:  
568 391–403.
- 569 42. Kutty, R. G., G. Xin, D. M. Schauder, S. M. Cossette, M. Bordas, W. Cui, and R. Ramchandran.  
570 2016. Dual specificity phosphatase 5 is essential for T cell survival. *PLoS One* 11: 1–16.
- 571 43. Indiveri, C., V. Iacobazzi, A. Tonazzi, N. Giangregorio, V. Infantino, P. Convertini, L. Console, and  
572 F. Palmieri. 2011. The mitochondrial carnitine/acylcarnitine carrier: Function, structure and  
573 physiopathology. *Mol. Aspects Med.* 32: 223–233.
- 574 44. van Duin, D., H. G. Allore, S. Mohanty, S. Ginter, F. K. Newman, R. B. Belshe, R. Medzhitov, and  
575 A. C. Shaw. 2007. Prevacine Determination of the Expression of Costimulatory B7 Molecules in  
576 Activated Monocytes Predicts Influenza Vaccine Responses in Young and Older Adults. *J. Infect. Dis.*  
577 195: 1590–1597.
- 578 45. Panda, A., F. Qian, S. Mohanty, D. van Duin, F. K. Newman, L. Zhang, S. Chen, V. Towle, R. B.  
579 Belshe, E. Fikrig, H. G. Allore, R. R. Montgomery, and A. C. Shaw. 2010. Age-Associated Decrease in  
580 TLR Function in Primary Human Dendritic Cells Predicts Influenza Vaccine Response. *J. Immunol.* 184:  
581 2518–2527.
- 582 46. Aldemir, H., V. Prod'homme, M.-J. Dumaurier, C. Retiere, G. Poupon, J. Cazareth, F. Bihl, and V.  
583 M. Braud. 2005. Cutting Edge: Lectin-Like Transcript 1 Is a Ligand for the CD161 Receptor. *J. Immunol.*  
584 175: 7791–7795.
- 585 47. Rosen, D. B., J. Bettadapura, M. Alsharifi, P. A. Mathew, H. S. Warren, and L. L. Lanier. 2005.  
586 Cutting Edge: Lectin-Like Transcript-1 Is a Ligand for the Inhibitory Human NKR-P1A Receptor. *J.*  
587 *Immunol.* 175: 7796–7799.
- 588 48. Kleinschek, M. A., K. Boniface, S. Sadekova, J. Grein, E. E. Murphy, S. P. Turner, L. Raskin, B.  
589 Desai, W. A. Faubion, R. de Waal Malefyt, R. H. Pierce, T. McClanahan, and R. A. Kastelein. 2009.  
590 Circulating and gut-resident human Th17 cells express CD161 and promote intestinal inflammation. *J.*  
591 *Exp. Med.* 206: 525–534.
- 592 49. Maggi, L., V. Santarlasci, M. Capone, A. Peired, F. Frosali, S. Q. Crome, V. Querci, M. Fambrini, F.  
593 Liotta, M. K. Levings, E. Maggi, L. Cosmi, S. Romagnani, and F. Annunziato. 2010. CD161 is a marker  
594 of all human IL-17-producing T-cell subsets and is induced by RORC. *Eur. J. Immunol.* 40: 2174–2181.
- 595 50. Cosmi, L., R. De Palma, V. Santarlasci, L. Maggi, M. Capone, F. Frosali, G. Rodolico, V. Querci, G.  
596 Abbate, R. Angeli, L. Berrino, M. Fambrini, M. Caproni, F. Tonelli, E. Lazzeri, P. Parronchi, F. Liotta, E.  
597 Maggi, S. Romagnani, and F. Annunziato. 2008. Human interleukin 17-producing cells originate from a  
598 CD161<sup>+</sup> CD4<sup>+</sup> T cell precursor. *J. Exp. Med.* 205: 1903–1916.
- 599 51. Gorenshteyn, D., E. Zaslavsky, M. Fribourg, C. Y. Park, A. K. Wong, A. Tadych, B. M. Hartmann, R.  
600 A. Albrecht, A. García-Sastre, S. H. Kleinstein, O. G. Troyanskaya, and S. C. Sealfon. 2015. Interactive  
601 Big Data Resource to Elucidate Human Immune Pathways and Diseases. *Immunity* 43: 605–614.
- 602 52. Cho, N. E., B. R. Bang, P. Gurung, M. Li, D. L. Clemens, T. M. Underhill, L. P. James, J. R. Chase,  
603 and T. Saito. 2016. Retinoid regulation of antiviral innate immunity in hepatocytes. *Hepatology* 63:  
604 1783–1795.
- 605 53. Furman, D., J. Chang, L. Lartigue, C. R. Bolen, F. Haddad, B. Gaudilliere, E. A. Ganio, G. K.  
606 Fragiadakis, M. H. Spitzer, I. Douchet, S. Daburon, J.-F. Moreau, G. P. Nolan, P. Blanco, J. Déchanet-  
607 Merville, C. L. Dekker, V. Jojic, C. J. Kuo, M. M. Davis, and B. Faustin. 2017. Expression of specific  
608 inflammasome gene modules stratifies older individuals into two extreme clinical and immunological  
609 states. *Nat. Med.* .
- 610 54. Darce, J. R., B. K. Arendt, X. Wu, and D. F. Jelinek. 2014. Regulated Expression of BAFF-Binding  
611 Receptors during Human B Cell Differentiation. *J. Immunol.* 179: 7276–7286.
- 612 55. Pockley, A. G., and B. Henderson. 2018. Extracellular cell stress (Heat shock) proteins—immune  
613 responses and disease: An overview. *Philos. Trans. R. Soc. B Biol. Sci.* 373.
- 614 56. Randow, F., and B. Seed. 2001. Endoplasmic reticulum chaperone gp96 is required for innate  
615 immunity but not cell viability. *Nat. Cell Biol.* 3: 891–896.
- 616 57. Mohanty, S., S. R. Joshi, I. Ueda, J. Wilson, T. P. Blevins, B. Siconolfi, H. Meng, L. Devine, K.  
617 Raddassi, S. Tsang, R. B. Belshe, D. a. Hafler, S. M. Kaech, S. H. Kleinstein, M. Trentalange, H. G.

- 618 Allore, and a. C. Shaw. 2014. Prolonged Proinflammatory Cytokine Production in Monocytes Modulated  
619 by Interleukin 10 After Influenza Vaccination in Older Adults. *J. Infect. Dis.* 211: 1174–1184.
- 620 58. Li, G., M. Yu, W. W. Lee, M. Tsang, E. Krishnan, C. M. Weyand, and J. J. Goronzy. 2012. Decline in  
621 miR-181a expression with age impairs T cell receptor sensitivity by increasing DUSP6 activity. *Nat. Med.*  
622 18: 1518–1524.
- 623 59. Kirkham, C. L., and J. R. Carlyle. 2014. Complexity and Diversity of the NKR-P1:Clr (Klrb1:Clec2)  
624 Recognition Systems. *Front. Immunol.* 5: 1–16.
- 625 60. Turtle, C. J., H. M. Swanson, N. Fujii, E. H. Estey, and S. R. Riddell. 2009. A Distinct Subset of Self-  
626 Renewing Human Memory CD8<sup>+</sup> T Cells Survives Cytotoxic Chemotherapy. *Immunity* 31: 834–844.  
627